Analytica Chimica Acta 1312 (2024) 342753

Contents lists available at ScienceDirect

Analytica Chimica Acta

journal homepage: www.elsevier.com/locate/aca

A rapid procedure for isotopic purification of copper and nickel from seawater using an automated chromatography system

Xiaopeng Bian [a,*], Shun-Chung Yang [a], Robert J. Raad [a], Nicholas J. Hawco [b], Jude Sakowski [c], Kuo-Fang Huang [d], Kyeong Pil Kong [a], Tim M. Conway [e], Seth G. John [a]

[a] Department of Earth Sciences, University of Southern California, Los Angeles, CA, USA
[b] Department of Oceanography, University of Hawai'i at Mānoa, Honolulu, HI, USA
[c] Elemental Scientific, Inc., Omaha, NE, USA
[d] Institute of Earth Sciences, Academia Sinica, Taipei, Taiwan
[e] College of Marine Science, University of South Florida, St. Petersburg, FL, USA

HIGHLIGHTS

- We develop a procedure for Ni–Cu isotopic analysis using automated chromatography.
- Nickel and Cu are fully recovered and cleanly separated from matrix elements.
- The method was tested on seawater samples and yielded accurate and precise data.
- The method may be adapted for the purification of Fe, Zn, and Cd in the future.

GRAPHICAL ABSTRACT

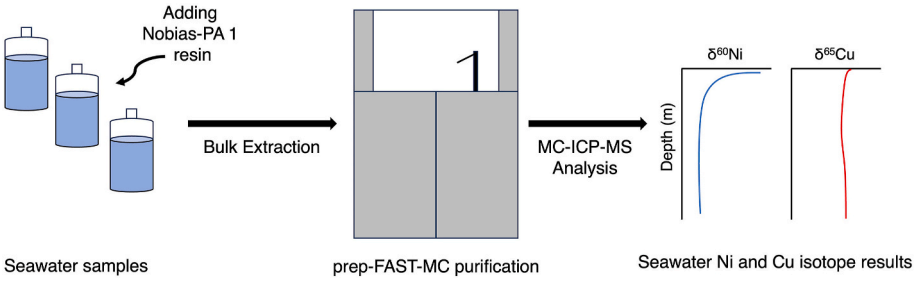

ARTICLE INFO

Handling Editor: Dr. L. Liang

Keywords:
Nickel
Copper
GEOTRACES
Ocean
Trace metals

ABSTRACT

Background: Trace metals such as iron, nickel, copper, zinc, and cadmium (Fe, Ni, Cu, Zn, and Cd) are essential micronutrients (and sometimes toxins) for phytoplankton, and the analysis of trace-metal stable isotopes in seawater is a valuable tool for exploring the biogeochemical cycling of these elements in the ocean. However, the complex and often time-consuming chromatography process required to purify these elements from seawater has limited the number of trace-metal isotope samples which can be easily processed in biogeochemical studies. To facilitate the trace-metal stable isotope analysis, here, we describe a new rapid procedure that utilizes automated chromatography for extracting and purifying Ni and Cu from seawater for isotope analysis using a prepFAST-MC™ system (Elemental Scientific Inc.).

Results: We have tested the matrix removal effectiveness, recoveries, and procedural blanks of the new purification procedure with satisfactory results. A nearly complete recovery of Ni and a quantitative recovery of Cu are achieved. The total procedural blanks are 0.33 ± 0.24 ng for Ni and 0.42 ± 0.18 ng for Cu, which is negligible for natural seawater samples. The new procedure cleanly separates Ni and Cu from key seawater matrix elements that may cause interferences during mass spectrometry analysis. When the new procedure was used to purify seawater samples for Ni and Cu stable isotope analysis by multi-collector ICP-MS, we achieved an overall uncertainty of 0.07 ‰ for δ^{60}Ni and 0.09 ‰ for δ^{65}Cu (2 SD). The new purification procedure was also tested using natural seawater samples from the South Pacific, for comparison of δ^{60}Ni and δ^{65}Cu achieved in the same

* Corresponding author. Department of Earth Sciences, University of Southern California, 3651 Trousdale Parkway, ZHS 117, Los Angeles, CA, 90089, USA.
E-mail address: xiaopenb@usc.edu (X. Bian).

https://doi.org/10.1016/j.aca.2024.342753
Received 10 February 2024; Received in revised form 16 April 2024; Accepted 20 May 2024
Available online 21 May 2024

samples purified by traditional hand columns. Both methods produced similar results, and the results from both methods are consistent with analyses of δ^{60}Ni and δ^{65}Cu from other ocean locations as reported by other laboratories.

Significance: This study presents a new rapid procedure for seawater stable-metal isotope analysis by automating the chromatography step. We anticipate that the automated chromatography described here will facilitate the rapid and accurate analysis of seawater δ^{60}Ni and δ^{65}Cu in future studies, and may be adapted in the future to automate chromatographic purification of Fe, Zn, and Cd isotopes from seawater.

1. Introduction

Trace metals such as Fe, Ni, Cu, Zn, and Cd are essential micronutrients for phytoplankton, influencing the marine ecosystem and global carbon and nitrogen cycles [1,2]. Metal stable isotope ratios in seawater including δ^{56}Fe, δ^{60}Ni, δ^{65}Cu, δ^{66}Zn, and δ^{114}Cd can provide valuable information about the sources, sinks, and cycling of trace metals in the ocean, and have advanced our understating of their biogeochemistry, especially with samples collected as part of the international GEOTRACES (geotraces.org) program [3,4]. Compared with δ^{56}Fe, δ^{66}Zn, and δ^{114}Cd measurements, data for seawater δ^{60}Ni and δ^{65}Cu remain relatively sparse, even though Ni and Cu are also essential micronutrients [4–12]. The scarcity of seawater Ni and Cu isotope data is partially due to analytical challenges in their isotope analysis—complex and time-consuming chromatographic purification processes are required, and the double spike technique is not applicable to Cu [13–17].

The first δ^{60}Ni analyses of modern seawater highlighted a lack of reasonable Ni isotope mass balance in the modern ocean, with most known sources being lighter than, but sinks being similar to, the average modern ocean δ^{60}Ni composition [5]; subsequent Ni isotope studies have advanced our understanding of this Ni mass balance issue [12,15,18–21]. Previous studies have also shown a near-homogenous deep ocean δ^{60}Ni (~+1.33 ‰), with only subtle fractionation of Ni isotope ratios towards the surface in oligotrophic regions (up to ~+1.75 ‰), indicating preferential uptake of lighter Ni isotopes by phytoplankton [12,14,16,22]. Seawater Cu isotope studies have been used to identify Cu sources to the ocean (e.g., atmospheric, riverine, and benthic input), and to explore marine processes which may fractionate Cu isotopes such as changes in oxidation state, biological uptake, and scavenging, while highlighting relatively little isotopic variability in deep water (~+0.6 ‰ to ~+0.7 ‰) [9,10,23–26]. For a recent comprehensive review of the isotope systematics of both elements in the oceans, readers are referred to Horner et al. [27].

When measuring Ni and Cu isotope ratios using multi-collector inductively coupled plasma mass spectrometry (MC-ICP-MS), an extraction and purification procedure is required to separate both elements from matrix elements to avoid spectral interferences (e.g., isobaric interferences, doubly charged ions, and polyatomic ions) and to minimize extreme matrix effects from the high salt matrix (e.g., blocked cones, signal suppression, and interferences) [28,29]. For both seawater Ni and Cu isotope analyses, a multi-step chromatography procedure is required [14,16,30], which is time-consuming, limiting the application of Ni and Cu isotope ratios as tracers in biogeochemical studies and leading to a paucity of data.

A commercially available prepFAST-MC™ system (Elemental Scientific Inc.) has previously been used to automate and facilitate the chromatography purification of many isotope systems, including Ca, Sr, Nd, Pb, Th, U, Pu, B, and Cu isotopes [31–36], and methods are in development for purification of Fe from seawater for δ^{56}Fe analysis [37]. Automated methods have several advantages compared with manual chromatography methods. For example, automated chromatography methods can facilitate higher sample throughput, which especially benefits projects with large sample numbers, such as the GEOTRACES program, as well as emerging medical research using stable metal isotopes [38–40]. Furthermore, automated methods can also allow for more consistent results by minimizing human sources of error.

Here, we present a new rapid procedure that utilizes automated chromatography for the purification of Ni and Cu from seawater for isotope analysis using the prepFAST-MC. Because previous literature does not generally describe the functioning of the prepFAST-MC in great depth, we also present detailed information about the prepFAST function and architecture, including valve plumbing, fluid flow, and instrument programming, which may benefit the future development of other automated methods. While this work focuses on methods for seawater Ni and Cu isotope analysis, we anticipate that the same purification protocols can be used for other types of samples, such as biological and geological materials. Moreover, although the procedure is designed for Ni and Cu isotope analysis, it shows promise for future adaptation to automate chromatographic purification of Fe, Zn, and Cd for isotope ratio analysis.

2. Materials and method development

2.1. Reagents and materials

All sample preparation work was carried out in flow benches with Ultra Low Particulate Air (ULPA) filtration in a class 100 clean lab in the Department of Earth Sciences at the University of Southern California (USC). Reagents used in this study include Aristar Ultra™ HF, HBr, H_2O_2, and NH_4OH, and TraceSELECT™ methanol (MeOH). Reagent grade HCl, HNO_3, and acetic acid (HAc) were purified by sub-boiling distillation in PFA distillation systems (Savillex DST-1000). All water used was ultrapure water (18.2 MΩ Milli-Q). Acid-cleaned PFA vials (Savillex®) were used for sample digestion and to dry down solutions. Acid-cleaned 15 mL low-density polyethylene (LDPE) VWR metal-free centrifuge tubes were used for sample loading and eluent collection on the prepFAST-MC™, and for subsequent sample storage for concentration and isotope analyses. The acid cleaning protocols are the same as those described in Conway et al. [17]. All clean equipment was handled with polyethylene gloves.

For the prepFAST chromatographic purification, columns with Bio-rad AG-MP1 resin (100–200 mesh) and Hitachi Nobias-PA1 resin were prepared in acid-cleaned 600 μL PFA column bodies obtained from Elemental Scientific Inc. (ESI). The AG-MP1 resin and Nobias-PA1 resin were cleaned by soaking in 10 % (v/v) HCl and 3 M HNO_3, respectively, for two weeks and stored in ultrapure water before use. The AG-MP1 column was filled with 300 μL AG-MP1 resin (a half-filled 600 μL column), and the Nobias-PA1 column was filled with 600 μL Nobias-PA1 resin.

2.2. Samples and standards

Seawater samples from the US GEOTRACES Pacific Meridional Transect (GP15) cruise and the SCOPE-Falkor cruise were used for method development and validation. GP15 samples were collected in the central Pacific basin aboard the R/V Roger Revelle along 152° W from 56° N to 20° S from 18 September to 24 November 2018, and Ni concentration data have been previously reported along the whole GP15 section [41]. Seawater samples were collected using the GEOTRACES Trace-element Carousel sampling system (GTC) using 12 L Teflon-coated GO-FLO bottles (General Oceanics) mounted on a Seabird rosette

system, deployed using a Dynacon winch with 7300 m of Vectran cable [42]. After collection, seawater was filtered from GO-FLO bottles through Acropak capsules (0.2 μm) into acid-washed 1 L LDPE bottles (Nalgene) in the GEOTRACES trace-metal clean van. The SCOPE-Falkor cruise was conducted in March/April 2018 in waters near Station ALOHA and the Hawaiian Islands. Seawater samples were collected from GO-FLO bottles attached to a polypropylene (Amsteel) line, and filtered through a 0.2 μm Acropak filter [43].

A multi-element standard (INORGANIC™ VENTURES IV-ICPMS-71A, a 10 μg mL^{-1} 43 Element ICP Calibration/Quality Control Standard, including Ag, Al, As, B, Ba, Be, Ca, Cd, Ce, Co, Cr, Cs, Cu, Dy, Er, Eu, Fe, Ga, Gd, Ho, K, La, Lu, Mg, Mn, Na, Nd, Ni, P, Pb, Pr, Rb, S, Se, Sm, Sr, Th, Tl, Tm, U, V, Yb, and Zn) was used to test the prepFAST-MC™ method, including the matrix element removal effectiveness, column yield, and blanks.

2.3. Metal extraction from seawater

Within several weeks to months after collection, seawater samples were acidified to a pH of ~1.8 via the addition of concentrated, distilled HCl (1 mL 12 N HCl/1 L seawater) in the clean lab at USC. At this time, H_2O_2 (30 %) was also added to each sample (1 mL H_2O_2/1 L seawater) to destroy strong copper-binding ligands [23]. After the acidification and addition of H_2O_2, seawater samples were stored for at least six months before Ni and Cu concentration analyses and three years before their isotope analyses.

Nickel and Cu concentrations were measured prior to isotope analyses in order to determine the amount of Ni double spike to be added to each sample, according to methods described in detail by Hawco et al. [44]. Briefly, 15 mL of acidified seawater was mixed with 50 μL of an isotope spike containing ^{57}Fe, ^{62}Ni, ^{65}Cu, ^{67}Zn, ^{207}Pb, and ^{110}Cd in an acid-washed 15 mL centrifuge tube. Using an automated seaFAST™ system, seawater was injected through a Nobias-PA1 column to preconcentrate trace metals away from the salt matrix. The sample was then eluted from the column using 0.5 mL 1 M HNO_3 containing 1 ng mL^{-1} In for metal concentration analysis using a Thermo Scientific Element 2 ICP-MS. Concentrations of Ni and Cu were calculated by isotope dilution.

After concentration analysis, 0.5–1 L of the acidified seawater sample was purified for Ni and Cu isotope analysis. First, a ^{61}Ni–^{62}Ni double spike containing 49.82 % ^{61}Ni and 49.09 % ^{62}Ni was added to achieve a spike/sample ratio of 1:1 (mol: mol) for Ni. Spiked seawater samples were then left to sit for one to three days to ensure equilibrium between sample and spike, followed by a bulk metal extraction process. The metal extraction process follows the protocol established by Conway et al. [17] and is briefly described below. Samples were amended with 2.5 mL pre-cleaned Nobias-PA1 resin and shaken vigorously for 2 h on a shaker table. Ammonium acetate (NH_4Ac) buffer and NH_4OH were then added to the seawater to adjust the pH to 6.0 ± 0.2, followed by shaking the sample for ~5 h. The resin was then recovered from the solution by filtering through an acid-washed, 3 μm polycarbonate filter (Whatman). After that, the resin was rinsed with 125 mL ultrapure water to remove salts, and metals were eluted with ~25 mL 3 M nitric acids into a 30 mL PFA beaker before evaporating to dryness on a hot plate overnight. Finally, samples were redissolved in 0.7 mL 11 M acetic acid +4 M HCl and transferred to 15 mL acid-cleaned LDPE centrifuge tubes for column purification using the prepFAST-MC™.

2.4. prepFAST-MC configuration and sample purification

The prepFAST-MC™ consists of an autosampler, two P6 valves (V1 and V2), one M10 stream selection valve, one P4 valve, a 13 mL sample loop, a 'vacuum' pumping system (named by ESI), four syringe pumps, and reagent bottles (Fig. 1). The P6 valve can be switched between the Load and Inject positions, and the P4 valve can be switched between Dispense and Fill positions (Fig. 1). The 13 mL sample loop is connected to the center connection port of the M10 valve, which can be connected to the other ten connection ports of the M10 valve to draw air/reagents into the loop or dispense air/reagents from the loop. The syringe pumps can move upwards (Fill) to draw air/reagents into the loop or downwards (Dispense) to push air/reagents out of the loop into waste or through the columns, and their speed can be controlled. A 'vacuum' pump (Fig. 1) does not operate by pulling a vacuum. Instead, it pumps reagent quickly through the system at a rate of approximately 5–20 mL min^{-1}, depending on the resistance of the tubing through which it discharges. The vacuum pump does not operate at a consistent flow rate or

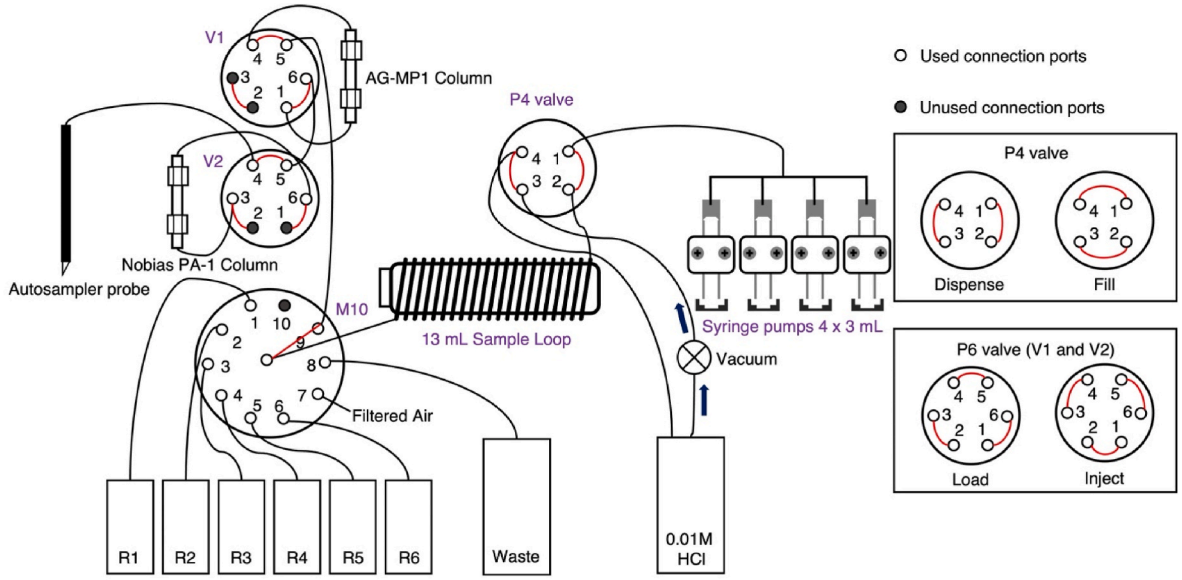

Fig. 1. Schematic diagram of the prepFAST-MC™ system. Red lines show connections inside the valves, and black lines show connections outside the valves. The V1 and V2 valves can switch between Load and Inject modes. The P4 valve can switch between Dispense and Fill modes. The M10 valve connects the center port with one of the ten radial positions. In this schematic diagram, the V1 and V2 valves are shown in Load mode, the P4 valve is shown in Dispense mode, and the M10 valve is connected to port 9. R1 to R6 represent six different reagents used in the Ni–Cu purification method (R1: 11 M HAc + 4 M HCl, R2: 5 M HCl, R3: 22 M methanol + 0.9 M HBr, R4: 1 M HF, R5: Milli-Q, R6: 2 M HNO_3).

high pressure, but is typically used to flush open lines.

The Ni–Cu prepFAST purification method used in this study is modified from the manual column method previously described by Yang et al. [16]. To evaluate the effectiveness of the prepFAST method, the same set of seawater samples was purified using both a previously-published hand column method [16] and prepFAST chromatography. The hand column and the prepFAST purification use the same set of reagents, but the reagent volumes differ due to the varying resin volumes in the hand and prepFAST columns. For the hand column purification, an AG-MP1 hand column (corresponding to the prepFAST AG-MP1-Ni-Cu step, Table 2) separated Ni, Cu, and Fe from each other. The Ni fraction was further purified with a Nobias-PA1 hand column (corresponding to the prepFAST Nobias-PA1-Ni step, Table 2) to separate Ni from the salt matrix, and the Cu fraction was further purified by a second AG-MP1 hand column (corresponding to the prepFAST AG-MP1-Cu step, Table 2) to separate Cu from interference elements.

Common prepFAST-MC™ operations are summarized in Table 1, and the prepFAST purification protocol for Ni and Cu isotopes is provided in Table 2. Briefly, the first AG-MP1 column (AG-MP1-Ni-Cu step, Table 2) separated various elements into three fractions—Ni fraction (eluted by 11 M HAc + 4 M HCl), Cu fraction (eluted by 5 M HCl) and FeZnCd fraction (eluted by 2 M HNO_3). The Ni fraction, after evaporation and redissolution in 0.7 mL of 0.05 M NH_4Ac, was further purified on the Nobias-PA1 column (Nobias-PA1-Ni step, Table 2) to separate Ni from salts. Similarly, the Cu fraction, after evaporation and redissolution in 0.7 mL of 22 M methanol +0.9 M HBr, was further purified on the second AG-MP1 column (AG-MP1-Cu step, Table 2) to separate Cu from the elements that may cause spectral interferences, including Ti, Mn, Cr, and S.

After both the hand-column and prepFAST chromatography procedures, the final Ni and Cu fractions were evaporated to dryness in 7 mL PFA vials, then redigested using 1 mL of 16 M HNO_3 and 0.1 mL of 30 % H_2O_2 at 160 °C for at least 6 h to decompose any leftover organic matter [45]. The samples were again evaporated to dryness and redissolved in 0.1 M HNO_3 to achieve a final concentration of approximately 100 ng mL^{-1} Ni and 100 ng mL^{-1} Cu for isotopic analysis.

2.5. Recovery and blank test

The prepFAST-MC™ processed multi-element standards and clean reagents to test the matrix removal effectiveness, the recoveries and blanks of Ni and Cu, and the memory effect of the prepFAST purification procedure. A testing standard solution was prepared by drying down the multi-element standard (described in Section 2.2) and redissolving it in 11 M HAc + 4 M HCl. Multi-element standards (~450 ng for all 43 elements) and blank samples (clean 11 M HAc + 4 M HCl) were purified alternately during the testing.

Table 1
Common prepFAST-MC™ operations.

The prepFAST-MC™ operations	V1 mode	V2 mode	M10 position	P4 valve mode	Syringe pump
Draw sample into the Sample Loop	Inject	Load	9	Dispense	Fill
Draw reagents into the Sample Loop	–	–	1 to 6	Dispense	Fill
Draw air into the Sample Loop	–	–	7	Dispense	Fill
Push reagents/sample from the Sample Loop through the AG-MP1 column to elute metals	Load	Load	9	Dispense	Dispense
Push reagents/sample from the Sample Loop through the Nobias-PA1 column to elute metals	Inject	Inject	9	Dispense	Dispense

Table 2
A summarized procedural outline for purification of Ni and Cu for MC-ICP-MS isotopic analysis by the prepFAST-MC™. The full procedure includes steps for rinsing tubing, Sample Loop, and the probe are not included here. A complete procedure with each command issued to the prepFAST-MC™ is provided in the Supplemental Material.

prepFAST Column	Step	Volume (μL)	Reagent	Syringe Speed (μL/min)
	Clean column	2000 × 2	2 M HNO_3	1000
	Rinsing	1000 × 1	Milli-Q Water	1000
AG-MP1-Ni-Cu	Condition column	500 × 2	11 M HAc + 4 M HCl	500
Column	Load sample and collect Ni	Sample volume	11 M HAc + 4 M HCl	500
	Elute Ni (for Nobias-PA1-Ni Column)	500 × 3	11 M HAc + 4 M HCl	500
	Elute Cu (for AG-MP1-Cu Column)	2000 × 3	5 M HCl	500
	Elute Fe, Zn, Cd	2000 × 3	2 M HNO_3	1000
	Clean column	2000 × 3	2 M HNO_3	1000
Nobias-PA1-Ni	Condition column	2000 × 2	Milli-Q Water	1000
Column	Load Sample	Sample volume	0.05 M NH_4Ac	500
	Elute salt	2000 × 3	Milli-Q Water	1000
	Elute Ni	2000 × 2	2 M HNO_3	1000
	Clean column	2000 × 1	2 M HNO_3	1000
	Rinsing	1000 × 1	Milli-Q Water	1000
AG-MP1-Cu	Condition column	500 × 2	22 M methanol + 0.9 M HBr	500
Column	Load Sample	Sample Volume	22 M methanol + 0.9 M HBr	500
	Elute interferences	1700 × 2	22 M methanol + 0.9 M HBr	500
	Elute Cu	2000 × 3	1 M HF or 5 M HCl	500
	Clean column	1700 × 3	2 M HNO_3	1000

To evaluate the recoveries of Ni and Cu during the first AG-MP1 column (AG-MP1-Ni-Cu column, Table 2), Ni, Cu, and FeZnCd fractions of multi-element standards were collected into 15 mL LDPE tubes. These three fractions were then dried down in clean PFA vials and redissolved in 1 mL of 0.1 M HNO_3 (containing 10 ng mL^{-1} In) before concentration analysis by Element 2 ICP-MS. The recovery of each element (e.g., Ni, Cu, Fe, etc.) was determined by summing its mass across all fractions and calculating its proportion in each fraction.

After the first AG-MP1 column, a Nobias-PA1 column further purified Ni from the salt matrix, and a second AG-MP1 column separated Cu from interfering elements. The recoveries of Ni and salt elements (e.g., Na, Mg, and Ca) of the Nobias-PA1 column were monitored by collecting and analyzing the salt fraction and Ni fraction; the recoveries of Cu and interference elements of the second AG-MP1 column were monitored by collecting and analyzing the interference fraction (eluted by 22 M methanol + 0.9 M HBr), Cu fraction, and the final column-cleaning HNO_3 fraction (Table 2 and Fig. 2).

Procedural blanks for the prepFAST purification were estimated for Ni and Cu by processing clean 11 M HAc +4 M HCl as samples. The Ni and Cu blanks for the first AG-MP1 column (AG-MP1-Ni-Cu step) were assessed by processing five blank samples. The Ni and Cu fractions were collected, dried down, and redissolved in 1 mL of 0.1 M HNO_3 with 10 ng mL^{-1} In before concentration analysis by the Element 2 ICP-MS. The total procedural blanks for Ni and Cu in the prepFAST purification were evaluated by processing five new blank samples through both the first AG-MP1 and Nobias-PA1 columns for Ni, and the first and second AG-

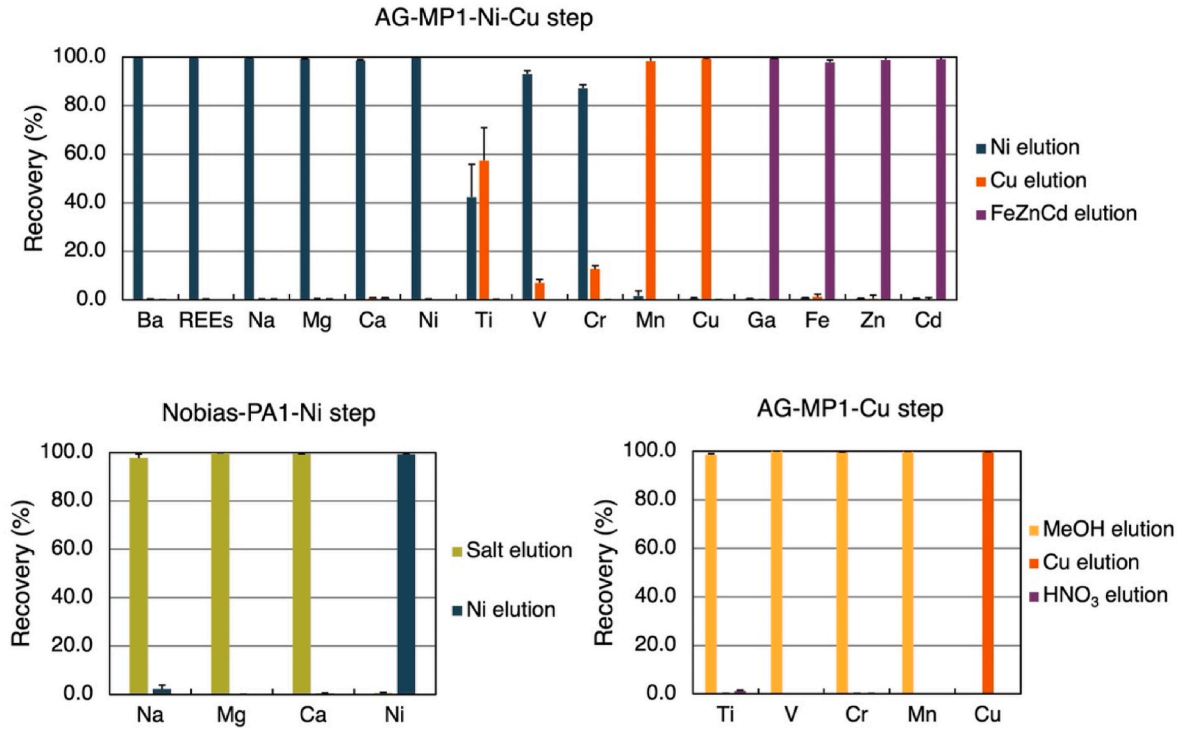

Fig. 2. Recovery of analyte elements and potential interference elements utilizing the prepFAST methods described here, with error bars representing 2σ.

MP1 columns for Cu. The final eluates of Ni and Cu were analyzed to determine the total procedural blanks.

The Ni blank for the Nobias-PA1 column (the second column for Ni purification) and the Cu blank for the AG-MP1-Cu column (the second column for Cu purification) were determined indirectly; they were evaluated by subtracting the Ni and Cu blanks of the first AG-MP1 column from the total procedural blanks (Table 6).

2.6. Isotopic analysis and data reduction

Analysis of δ^{60}Ni and δ^{65}Cu was conducted using a Thermo Neptune Plus MC-ICP-MS at either USC or the University of South Florida (USF). A PFA nebulizer with a flow rate of 100–120 μL min^{-1} and the Apex 2Q desolvation system were used to introduce samples for Ni isotope analysis. The same PFA nebulizer and a quartz cyclonic/Scott double-pass spray chamber were used to introduce samples for Cu isotope analysis. In each case, the Neptune was operated in 'high-resolution' mode while measuring Ni and Cu isotopes to resolve potential polyatomic interferences. In particular, when we tuned the Neptune for Cu isotope analysis, we used a pure 1 μg mL^{-1} Na solution to monitor the peak shape of ^{63}Cu and observed the interference of ^{23}Na^{40}Ar^{+} on ^{63}Cu. We then analyzed Cu isotopes on the interference-free plateau, even though no interference was observed in purified samples.

The cup configurations for Ni and Cu isotope analysis are listed in Table 3. For Ni isotope analysis, ^{58}Ni, ^{60}Ni, ^{61}Ni, and ^{62}Ni were simultaneously measured, along with monitoring ^{57}Fe to correct for any interference of ^{58}Fe on ^{58}Ni. For Cu isotope analysis, ^{63}Cu, ^{65}Cu, and two gallium (Ga) isotopes (^{69}Ga and ^{71}Ga) were measured simultaneously. Gallium isotopes were measured as the internal standard to correct for instrumental mass bias of Cu.

After Ni isotope analysis, we recalculated Ni concentrations of the GP15 samples using the isotope dilution technique based on on-peak blank, interference, and mass-bias corrected ^{62}Ni/^{60}Ni ratios analyzed by the Neptune. The recalculated Ni concentrations ([Ni]) agree well with the GP15 Ni concentration data previously reported [41]—the differences in [Ni] between the two datasets are less than 2.1 % (Table S1)—and are used in this study when we present GP15 Ni concentrations (Fig. 3).

For δ^{60}Ni, a double spike technique was used to correct for instrumental mass bias and any potential Ni isotope fractionation during sample purification. The data reduction scheme followed the iterative approach described by Siebert et al. [46]. We express Ni isotope ratios using the conventional delta notation compared to the NIST 986 Ni isotope standard:

$$\delta^{60}Ni = \left[\left({}^{60}Ni/{}^{58}Ni \right)_{sample} \Big/ \left({}^{60}Ni/{}^{58}Ni \right)_{NIST986} - 1 \right] \times 1000 \quad (1)$$

Copper has only two stable isotopes, so the double spike technique is not applicable. Here, a combination of internal standardization and external standard sample bracketing (SSB) technique was used for mass bias correction on Cu isotope ratios [29]. Gallium was added to Cu isotope samples as the internal standard at a Ga:Cu concentration ratio of 2:1. The mass bias correction factor of Cu is not identical to that of Ga, so a 'regression' internal standardization method was used to correct for the instrumental mass bias of Cu by monitoring the linear relationship between the mass bias correction factors of Cu and Ga [29]. After that, the SSB technique was used to calculate the Cu isotopic compositions of samples by analyzing samples and Cu standards alternately. Copper isotope results are expressed in delta notation relative to the NIST 976

Table 3
Cup configurations for Ni and Cu isotope analysis.

Faraday Cup position	L4	L3	L2	L1	C	H1	H2	H3	H4
Ni cup configuration		^{57}Fe	^{58}Ni		^{60}Ni	^{61}Ni	^{62}Ni		
Cu cup configuration		^{63}Cu		^{65}Cu		^{69}Ga		^{71}Ga	

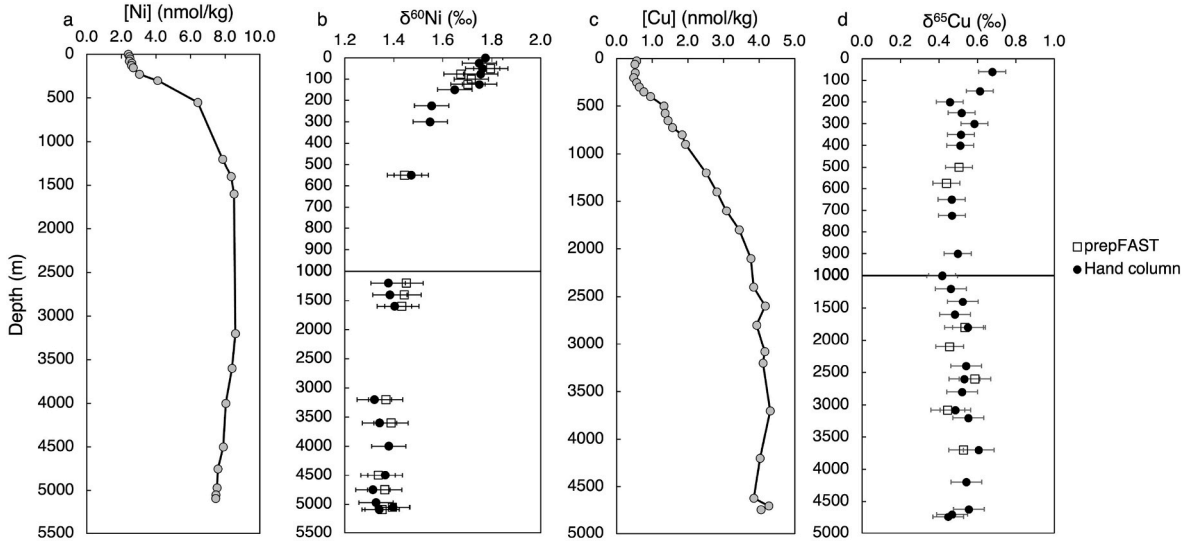

Fig. 3. Nickel concentration (a) and stable isotope (b) profiles for samples collected on the GP15 transect in the South Pacific (10.5° S, 152° W). Copper concentration (c) and stable isotope (d) profiles for GP15 samples in the South Pacific (15° S, 152° W). For Ni and Cu isotope data, white squares are results obtained using the prepFAST-MC method, while black circles represent samples purified using the manual column method. Error bars are external precision (2σ) during the isotope analysis (0.07 ‰ for both δ^{60}Ni and δ^{65}Cu). Note that the upper 1000 m depth range is expanded for δ^{60}Ni and δ^{65}Cu profiles, while not for Ni and Cu concentration profiles.

Cu isotope standard:

$$\delta^{65}Cu = \left[\left({}^{65}Cu/{}^{63}Cu \right)_{sample} \Big/ \left({}^{65}Cu/{}^{63}Cu \right)_{NIST976} - 1 \right] \times 1000 \qquad (2)$$

3. Results and discussion

3.1. Interferences and matrix removal

Spectral interferences can influence Ni and Cu isotope analysis, yielding inaccurate results [16,47,48]. Because Ga is used as the internal standard for Cu isotope analysis, spectral interferences on Ga isotopes are also considered here. Among all the measured Ni (^{58}Ni, ^{60}Ni, ^{61}Ni, and ^{62}Ni), Ga (^{69}Ga and ^{71}Ga), and Cu (^{63}Cu and ^{65}Cu) isotopes, the only relevant isobaric interference is from ^{58}Fe interfering with ^{58}Ni. However, multiple isotopes may be impacted by interferences from polyatomic/doubly charged ions. The important interferences on Ni, Ga, and Cu isotopes are summarized in Table 4. For Ni and Cu isotopes, many polyatomic interferences contain Na, Mg, and Ca, which are abundant in seawater and ubiquitous in biological and geological samples [49,50]. Some polyatomic interferences can be separated from target isotopes using high resolution (HR) resolving power in MC-ICP-MS analysis. Methods are well-established for the analysis of Fe isotopes using a Neptune MC-ICP-MS, which rely on the optical separation of $^{56}Fe^{+}$ from $^{40}Ar^{16}O^{+}$ at a Neptune resolving power of at least 4000 (medium resolution) but for seawater Fe typically around 9000–11000 in high-resolution mode, which is close to the limit of the resolving power of the Neptune MC-ICP-MS [17,51,52]. Thus, with current HR slit widths, the Neptune is unlikely to be able to resolve any polyatomic interferences which require a resolution significantly greater than that is required to separate $^{56}Fe^{+}$ from $^{40}Ar^{16}O^{+}$; however, many relevant interferences for the analysis of Ni and Cu isotopes do indeed require much higher resolution to resolve (Table 4), and therefore it is necessary to quantitatively separate the matrix elements (e.g., Na, Mg, Ca) from Ni and Cu prior to analysis using chromatography methods [14,16,30].

In our procedure, Ni, Cu, and Fe are separated from each other quantitatively in the prepFAST AG-MP1-Ni-Cu column step, so that the interference of ^{58}Fe on ^{58}Ni is effectively eliminated (although still monitored and corrected for during analysis). Matrix elements such as Na, Mg, and Ca are separated from Ni and Cu through multiple steps.

Table 4
Main interferences on Ni, Cu, and Ga isotopes (modified from Enge et al., 2016; Gall et al., 2012; May and Wiedmeyer, 1998; Petit et al., 2008) [32,48,62,63].

Isotope	Interferences	Theoretical mass resolution (m/Δm)[a]
^{63}Cu	$^{23}Na^{40}Ar^{+}$	2736
	$^{23}Na^{40}Ca^{+}$	2736
	$^{25}Mg^{38}Ar^{+}$	3312
	$^{47}Ti^{16}O^{+}$	3702
	$^{49}Ti^{14}N^{+}$	2997
^{65}Cu	$^{130}Ba^{++}$	2597
	$^{25}Mg^{40}Ar^{+}$	3092
	$^{48}Ti^{16}O^{1}H^{+}$	2823
	$^{49}Ti^{16}O^{+}$	4329
^{58}Ni	$^{58}Fe^{+}$	28967
	$^{116}Cd^{++}$	3311
	$^{23}Na^{35}Cl^{+}$	2414
	$^{40}Ar^{18}O^{+}$	2146
	$^{40}Ca^{18}O^{+}$	2146
	$^{42}Ca^{16}O^{+}$	3049
^{60}Ni	$^{23}Na^{37}Cl^{+}$	2397
	$^{44}Ca^{16}O^{+}$	3154
	$^{24}Mg^{36}Ar^{+}$	2724
^{61}Ni	$^{25}Mg^{36}Ar^{+}$	2649
	$^{45}Sc^{16}O^{+}$	3047
^{62}Ni	$^{46}Ti^{16}O^{+}$	3096
	$^{44}Ca^{18}O^{+}$	2382
	$^{26}Mg^{36}Ar^{+}$	2693
^{69}Ga	$^{138}Ba^{++}$	2336
	$^{53}Cr^{16}O^{+}$	5302
	$^{51}V^{18}O^{+}$	3446
	$^{68}Zn^{1}H^{+}$	6892
	$^{55}Mn^{14}N^{+}$	3829
^{71}Ga	$^{55}Mn^{16}O^{+}$	8866

[a] m is the mass of the target isotope (in atomic mass units, AMU), and Δm is the mass difference (in AMU) between the target isotope and the interference. Note that the theoretical mass resolution (m/Δm) required to separate $^{56}Fe^{+}$ from $^{40}Ar^{16}O^{+}$ is 2432; a m/Δm much greater than 2432 (for example, greater than 3000) likely exceeds the resolving power of Neptune MC-ICP-MS.

First, most of Na, Mg, and Ca (>99 %) are removed in the bulk extraction step using the Nobias-PA1 resin [16,17]. Any Na, Mg, and Ca that are still present from bulk extraction are co-eluted with Ni and separated from Cu in the AG-MP1-Ni-Cu column step, and do not cause interferences during the analysis of Cu isotopes. Following the

AG-MP1-Ni-Cu column step, further effective separation of Na, Mg, and Ca from Ni was achieved in the Nobias-PA1 column step (Fig. 2 and Table 5).

Gallium is used as the internal standard for Cu isotope analysis, so it is also important to effectively separate any sample Ga from Cu. We find that Ga is separated from Cu in the AG-MP1-Ni-Cu step. Furthermore, the primary elements that may cause interferences on Ga isotopes, such as Ba, Cr, V, Zn, and Mn, are also cleanly removed from the final Cu fraction during the AG-MP1-Ni-Cu step and the AG-MP1-Cu step (Fig. 2 and Table 5).

Polyatomic Ti species also yield interferences on both ^{63}Cu and ^{65}Cu, as well as on ^{62}Ni (Table 4). The influence of Ti on seawater Ni and Cu isotope analysis is likely to be negligible because of the low concentration of dissolved Ti in seawater (0 pM to several hundreds of pM) [53]. However, for samples with high Ti concentrations (e.g., geological samples), it is prudent to separate Ni and Cu from Ti before Ni and Cu isotope analysis. Below we suggest some modifications to our current prepFAST method to achieve this goal for high-Ti samples. In the prepFAST method presented here, in the AG-MP1-Ni-Cu step, 42 % of Ti is eluted in the Ni fraction and 57 % in the Cu fraction, respectively. Titanium in the Cu fraction is further separated from Cu during the AG-MP1-Cu step, but Ti in the Ni fraction cannot be separated from Ni during the Nobias-PA1-Ni step (Fig. 2 and Table S3). In order to better separate Ti from Ni and Cu, in the AG-MP1-Ni-Cu step, the reagent to elute Ni can be changed from 11 M HAc +4 M HCl to 15 M HAc +1.2 M HCl so that Ti can be removed from the Ni fraction more effectively, and Ti eluted in the Cu fraction will be further separated from Cu in the AG-MP1-Cu step [16]. We also note that in the AG-MP1-Cu step, most Ti (>98 %) is eluted by 22 M methanol + 0.9 M HBr (Fig. 2 and Table S3), so the use of 1 M HF to retain Ti on the column when eluting Cu is unnecessary [16]. In the AG-MP1-Cu step, the 1 M HF used to elute Cu can be replaced by 5 M HCl, the same as in the AG-MP1-Ni-Cu step, to avoid the use of HF.

To further evaluate the effectiveness of the whole purification procedure—including both the bulk extraction and the prepFAST purification—we analyzed the content of the matrix elements in the final purified Ni and Cu fractions of seawater samples from the US GEOTRACES GP15 cruise using an Agilent 8900 triple-quadrupole ICP-MS. All the interference matrix elements are cleanly separated from Ni and Cu (Table 5). In the final purified Cu fractions, Na has the highest yet still insignificant concentrations among the interference matrix elements, with an average value of 22.5 ng mL^{-1} and a median value of 19.4 ng mL^{-1}, much lower than Cu concentrations (about 100 ng mL^{-1}) (Table 5). In the final purified Ni fractions, Ca has the highest concentration among Na, Mg, and Ca, with an average value of 74.7 ng mL^{-1} and a median value of 51.4 ng mL^{-1}, lower than Ni concentrations (about 100 ng mL^{-1}), and negligible compared with the amount of Ca in 1 L seawater (about 400 mg). Among the calcium isotopes (^{40}Ca, ^{42}Ca, and ^{44}Ca) that may form calcium oxide interferences on Ni isotopes (Table 4), ^{40}Ca has the highest relative abundance of 96.94 %; the interference of $^{40}Ca^{18}O^{+}$ on $^{58}Ni^{+}$ can be well resolved using the high resolution of the Neptune. With a Ca concentration lower than Ni and the use of the dry plasma condition to minimize the yield of oxides (typically less than 1 %) [54,55], the influence of Ca oxides from the other two minor Ca isotopes (^{42}Ca and ^{44}Ca) on Ni isotopic analysis is negligible. Therefore, after the whole purification procedure, all matrix elements that might introduce interferences on Ni and Cu isotopic analyses are effectively removed.

Table 5
Concentrations of matrix elements in the final purified Ni and Cu fractions of seawater samples (ng mL^{-1}).

Elements	Cu solutions (n = 35)		Ni solutions (n = 45)	
	Average±1SD	Median	Average±1SD	Median
Na	22.5 ± 13.1	19.4	28.7 ± 15.4	28.1
Mg	1.8 ± 1.1	1.4	37.2 ± 17.2	38.3
Al	3.8 ± 3.8	2.3	5.5 ± 3.0	4.9
P	10.8 ± 13.5	5.2	31.3 ± 14.8	31.6
Ca	11.4 ± 11.5	7.4	74.7 ± 57.1	51.4
Ti	0.3 ± 0.9	0.1	0.1 ± 0.1	0.1
V	0.0 ± 0.0	0.0	15.4 ± 22.6	3.6
Cr	0.1 ± 0.1	0.1	0.1 ± 0.1	0.1
Mn	0.1 ± 0.0	0.0	0.2 ± 0.8	0.1
Fe	5.4 ± 5.4	4.6	0.3 ± 1.1	−0.1
Co	0.0 ± 0.0	0.0	0.0 ± 0.1	0.0
Ni	0.0 ± 0.0	0.0	90.9 ± 12.6	91.8
Cu	103.7 ± 10.2	103.2	0.9 ± 3.9	0.1
Zn	18.4 ± 25.9	8.4	2.1 ± 9.8	0.5
Mo	8.2 ± 9.9	5.4	0.9 ± 0.6	0.8
Cd	0.0 ± 0.1	0.0	0.0 ± 0.0	0.0
Ba	0.0 ± 0.1	0.0	0.0 ± 0.0	0.0
La	0.0 ± 0.0	0.0	0.1 ± 0.1	0.1
Ce	0.0 ± 0.0	0.0	0.0 ± 0.0	0.0
Pr	0.0 ± 0.0	0.0	0.0 ± 0.0	0.0
Nd	0.0 ± 0.0	0.0	0.1 ± 0.1	0.1
Pb	2.6 ± 3.2	1.1	0.2 ± 0.1	0.1

3.2. Recoveries and column life

In this procedure, Cu isotopes were analyzed using the standard sample bracketing method because the double spike technique is not applicable [56,57]. Thus, a quantitative recovery of Cu is required throughout the purification procedure to avoid potential isotope fractionation. Nickel isotopes were analyzed using the double spike technique so a quantitative recovery is not required [57], but a higher recovery is preferred.

In this study, we evaluated the recoveries of Ni and Cu in both the bulk extraction and prepFAST purification steps. The recoveries of Ni and Cu during the bulk extraction step have been previously reported; Conway et al. observed recoveries of 92 ± 14 % (2SD) for Ni and 80 ± 2 % (2SD) for Cu [17], and Yang et al. reported 102 ± 3 % (2SD) for Ni and 86 ± 3 % (2SD) for Cu [16]. The incomplete recovery of Cu in these studies may be attributed to the presence of inert Cu which is tightly bound by strong organic ligands and resistant to extraction by Nobias-PA1 resin. To address this, in this study, we added H_2O_2 to seawater samples and stored them for at least three years before Cu isotopic analysis in order to oxidize and break down strong copper-binding ligands, as discussed in prior work. Previous studies have shown that inert Cu can be effectively recovered by adding H_2O_2 to acidified seawater samples and storing them for 4 months [23], or by storing acidified seawaters for more than 4 years even without the addition of H_2O_2 [9,58].

We further evaluated the recoveries of Ni and Cu during the Nobias bulk extraction step by analyzing Ni and Cu concentrations in post-extraction seawater using a seaFAST procedure (described in Section 2.3). In the post-bulk extraction seawater, the average Ni concentration is 0.18 ± 0.04 nM (2SE, n = 45), and the average Cu concentration is 0.00 ± 0.06 nM (2SE, n = 45), indicating a nearly complete recovery of Ni and a quantitative recovery of Cu.

During the prepFAST purification, both Ni and Cu were quantitatively recovered. During the purification by the first AG-MP1 column (AG-MP1-Ni-Cu step, Table 2), 99.8 ± 0.2 % (2SD, n = 5) of Ni and 99.3 ± 0.3 % (2SD, n = 5) of Cu were collected in their respective fractions (Fig. 2 and Table 6). Nickel was then effectively separated from the salt matrix (e.g., Na, Mg, Ca) in the Nobias-PA1-Ni step, with a recovery of 99.4 ± 0.2 % (2SD, n = 5). Similarly, Cu was further separated from Ti, V, Cr, and Mn in the AG-MP1-Cu step, with a recovery of 99.9 ± 0.0 % (2SD, n = 5) (Fig. 2 and Table 6). These results demonstrate that the prepFAST purification process achieves quantitative recoveries for both Ni and Cu. Overall, by combining the bulk extraction with the prepFAST purification, the whole purification procedure yields a nearly complete recovery of Ni and a quantitative recovery of Cu.

During method development, the same prepFAST columns were used for more than 400 standards/samples, and consistent yields were

Table 6
The recoveries and procedural blanks of Ni and Cu during the prepFAST purification.

	Ni Recovery	Cu Recovery	Ni blank	Cu blank
AG-MP1-Ni-Cu Step	99.8 ± 0.2 % (2SD, n = 5)	99.3 ± 0.3 % (2SD, n = 5)	0.08 ± 0.02 ng (2SD, n = 5)	0.18 ± 0.07 ng (2SD, n = 5)
Nobias-PA1-Ni Step	99.4 ± 0.2 % (2SD, n = 5)	n.d.	0.16 ± 0.05 ng[a]	n.d.
AG-MP1-Cu Step	n.d.	99.9 ± 0.0 % (2SD, n = 5)	n.d.	0.16 ± 0.16 ng[a]
Total recoveries and procedural blanks of the prepFAST purification[b]	99.2 ± 0.3 %(2SD)	99.2 ± 0.3 % (2SD)	0.24 ± 0.05 ng (2SD, n = 5)	0.34 ± 0.15 ng (2SD, n = 5)

[a] The Ni blank of the Nobias-PA1-Ni Step and the Cu blank of the AG-MP1-Cu Step were calculated by subtracting the Ni and Cu blanks of the first AG-MP1 column from the total prepFAST procedural blanks.

[b] The total procedural blanks of the whole purification procedure are 0.33 ± 0.24 ng for Ni and 0.42 ± 0.18 ng for Cu, greater than the blanks of the prepFAST purification. See Section 3.3 for details.

achieved, indicating that the lifespan of the columns is long, at least 400 samples. Furthermore, another automated seawater trace metal concentration analysis system (ESI seaFAST™) also uses columns packed with Nobias-PA1 resin and can purify hundreds of seawater samples before exhausting the column [59]. As such, the same columns can be used for large sample sets. When the columns are approaching the end of their lifecycle, the resin degradation is expected to decrease Ni and Cu yields. It may therefore be helpful to monitor column performance when running natural samples by systematically processing an isotope reference material with samples, as has been recommended previously [32].

3.3. Blanks and sample carryover

In order to evaluate the total procedural blanks of the whole purification procedure, we combined the bulk extraction blanks with the prepFAST purification blanks. The blanks of Ni and Cu during the bulk extraction step were previously reported [17], with a Ni blank of 0.09 ± 0.24 ng (2SD) and a Cu blank of 0.08 ± 0.10 ng (2SD). For the prepFAST purification, in the AG-MP1-Ni-Cu step, the procedural blanks were 0.08 ± 0.02 ng (2SD, n = 5) for Ni and 0.18 ± 0.07 ng (2SD, n = 5) for Cu in their respective fractions. The total procedural blanks for the prepFAST purification were 0.24 ± 0.05 ng for Ni (2SD, n = 5) and 0.34 ± 0.15 ng for Cu (2SD, n = 5) (Table 6). When combining the blanks from the bulk extraction and the prepFAST purification, for the whole purification procedure, the Ni blank is 0.33 ± 0.24 ng and the Cu blank is 0.42 ± 0.18 ng (Table 6).

These total procedural blanks are negligible relative to the amount of Ni and Cu in 1 L open ocean seawater—roughly 100–600 ng Ni and 30–250 ng Cu—and have minimal impact on analytical uncertainty. The total Ni procedure blank accounts for <0.3 % of the total Ni, and <1.4 % of Cu in seawater samples. Assuming the δ^{60}Ni and δ^{65}Cu of blanks are similar to the continental crust, they are about 1.3 ‰ lighter than seawater δ^{60}Ni, and 0.6 ‰ lighter than seawater δ^{65}Cu [9,12,60,61]. A contribution of 0.3 % Ni from blanks will decrease the analyzed seawater δ^{60}Ni value by 0.0039 ‰, and a contribution of 1.4 % Cu from blanks will decrease the analyzed seawater δ^{65}Cu by 0.0084 ‰. Both are less than 0.01 ‰ and thus negligible.

Sample carryover was also tested alongside the testing of procedural blanks. Alternate processing of blank samples and multi-element standards (containing ~450 ng Ni and Cu) on the prepFAST-MC did not lead to any significant increase in blanks.

3.4. Method validation using natural seawater samples

The whole purification procedure effectively removes all matrix elements from seawater in the final purified Ni and Cu fractions (Table 5 and Section 3.1). To further validate the whole purification procedure, we purified seawater samples from the US GEOTRACES GP15 cruise using both the manual method [16] and the new prepFAST purification described here. The results of the two methods are consistent with each other when considering analytical uncertainties (Fig. 3).

Seawater samples from 10.5° S, 152° W in the South Pacific were analyzed for dissolved Ni concentrations and δ^{60}Ni (Fig. 3, Table S1). In these samples, Ni exhibits a typical nutrient-type profile, with lower concentrations in surface seawater and higher concentrations in deep seawater [41]. The average Ni isotope composition of deep waters below 3000 m is +1.36 ± 0.05 ‰ (2SD, n = 14, Fig. 3), consistent with the deep water δ^{60}Ni found in other ocean regions [12,14], while δ^{60}Ni increases towards the surface (Fig. 3). This increase in δ^{60}Ni towards the surface can be interpreted as reflecting the preferential uptake of lighter Ni isotopes by phytoplankton, as for similar patterns observed in other oceanic regions including the South Pacific subtropical gyre, the North Pacific subtropical gyre, the Eastern Tropical North Pacific, and the South Atlantic [11,12,14,16]. Notably, however, the new data in this study include the heaviest surface seawater Ni isotope value yet reported (δ^{60}Ni = +1.80 ‰), even though the surface Ni concentration (2.40 nmol/kg) is higher than typical oligotrophic surface seawater Ni concentrations (~2 nmol/kg). Thus, the Ni isotope dataset presented here provides intriguing information about global Ni isotope systematics, which we plan to interpret in the future using additional δ^{60}Ni data generated with this method.

Seawater samples from 15° S, 152° W in the South Pacific were analyzed for Cu concentrations and isotopes (Fig. 3, Table S2). Copper concentrations increase nearly linearly with depth to ~3000 m. Below 3000 m, Cu concentrations change little with depth (Fig. 3). Copper isotope values slightly decrease with depth from the surface to 200 m and are homogeneous below 200 m (δ^{65}Cu values range from +0.42 ‰ to +0.61 ‰). The average Cu isotope value below 1000 m is +0.51 ± 0.10 ‰ (2SD, n = 20), which is slightly lighter than previously reported δ^{65}Cu in the South Pacific and South Atlantic [9,14,24]. At 30° S, 165° E (South Pacific), the average seawater δ^{65}Cu value between 1000 m and 3000 m is +0.62 ± 0.09 ‰ (2SD, n = 5) [24]. At 30° S, 170° W (South Pacific), seawater δ^{65}Cu values vary between +0.56 ‰ and +0.65 ‰ at depths between 400 m and ~5200 m [14]. At ~40° S in the South Atlantic, seawater δ^{65}Cu values vary between ~+0.6 ‰ to ~+0.7 ‰ below 2000 m [9]. The δ^{65}Cu values in this study for samples from 15° S are slightly lighter than for samples collected at 30° S and 40° S, which may reflect the continuation of a trend that deep seawater δ^{65}Cu values decrease northwards (from 46° S to 30° S) in the South Pacific [24]. The δ^{65}Cu data reported here will also be interpreted in greater detail in forthcoming work, utilizing additional data from samples processed with the methods described here.

3.5. Analytical precision and uncertainty

We evaluated the reproducibility of Ni and Cu isotopic analysis by repeatedly analyzing pure isotope standards at both USC and USF. Two Ni isotope standards, 100 ppb Wako Ni and 100 ppb VWR Ni (spiked with Ni double spikes at a standard: spike ratio of 1: 1), and a Cu isotope standard (100 ppb NIST SRM 3114 Cu) were used. Repeated analysis of them over the last 3 years yields an average value of −0.28 ± 0.07 ‰ (2SD, n = 75) for Wako Ni, +0.42 ± 0.07 ‰ (2SD, n = 113) for VWR Ni, and −0.06 ± 0.07 ‰ (2SD, n = 344) for NIST 3114 Cu. These results are consistent with published values [14,16,23], and show that the external precision of isotopic analysis by Neptune is 0.07 ‰ for both δ^{60}Ni and δ^{65}Cu.

To test the repeatability of the prepFAST method for Ni isotope analysis, a single 4 L surface seawater sample collected in the North

Pacific Subtropical Gyre (24.35° N, 160.52° W, ~60 m) was split into ten samples after bulk extraction, and then separately purified by the prepFAST and analyzed by MC-ICP-MS at USF. The average δ^{60}Ni value of the surface seawater sample is +1.56 ± 0.04 ‰ (2SD, n = 10) (Fig. 4). We further evaluated the stability of the prepFAST method using deep seawater samples collected between 1000 m and 3000 m at two stations (47° N, 152° W and 52° N, 152° W) from the GP15 cruise in the North Pacific. These samples share the same water mass—Pacific Deep Water (PDW). Therefore, although the PDW samples were collected at different depths and latitudes, we expect them to have identical δ^{60}Ni and δ^{65}Cu. The PDW samples were purified by prepFAST and analyzed by MC-ICP-MS for δ^{60}Ni and δ^{65}Cu at USF. The analysis of the PDW samples quantifies the upper bound of the external precision of the prepFAST method. The average δ^{60}Ni value of the PDW samples is +1.33 ± 0.07 ‰ (2SD, n = 19), and their average δ^{65}Cu value is +0.42 ± 0.09 ‰ (2SD, n = 19) (Fig. 4). Based on these results, we regard a conservative estimate of the uncertainty associated with the whole purification and analytical procedure to be 0.07 ‰ for δ^{60}Ni and 0.09 ‰ for δ^{65}Cu.

The uncertainty in the seawater δ^{60}Ni and δ^{65}Cu values obtained from the purification procedure presented in this study is impacted by several factors, including inter-sample variability, procedural blanks, interference from matrix elements, and precision of the instrument. We quantified the uncertainty using PDW seawater samples. Although these samples share the same water mass and are expected to have the same δ^{60}Ni and δ^{65}Cu values, they may not be identical. Procedural blanks and matrix elements have minimal effects on analytical uncertainty (<0.01 ‰), as discussed in Sections 3.1 and Section 3.3. Thus, the precision of the instrument (Neptune MC-ICP-MS) constitutes a major proportion of the uncertainty. During isotopic analysis, the external precision is 0.07 ‰ for both δ^{60}Ni and δ^{65}Cu. These values match the overall uncertainty of seawater δ^{60}Ni and δ^{65}Cu values, which are 0.07 ‰ and 0.09 ‰, respectively. Overall, the purification procedure presented in this study facilitates rapid, accurate, and precise Ni and Cu isotopic analysis in seawater samples.

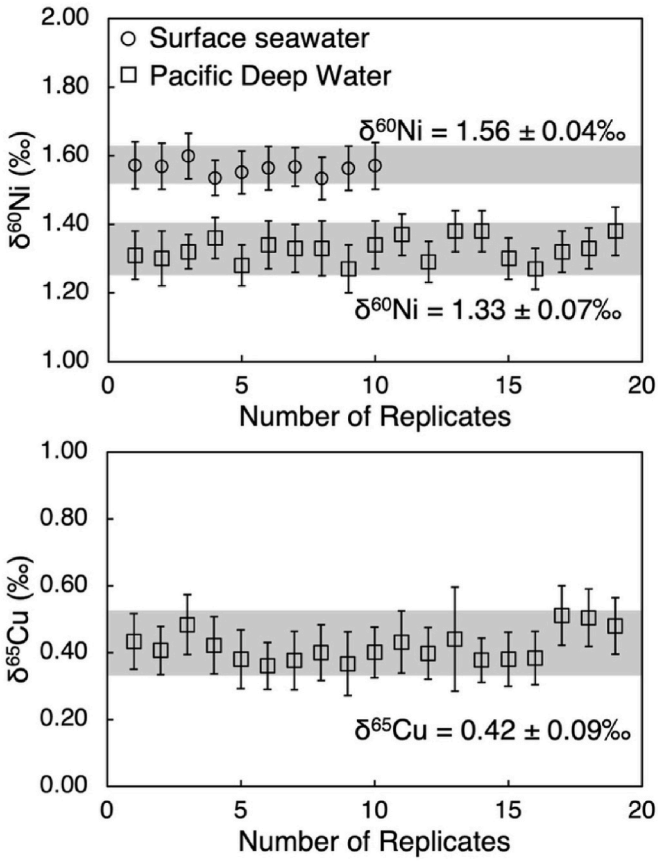

Fig. 4. External reproducibility for δ^{60}Ni and δ^{65}Cu based on repeated purification by prepFAST and analysis of the same original seawater sample. The surface seawater δ^{60}Ni data were obtained from a single 4 L surface seawater sample collected in the North Pacific. The deep water δ^{60}Ni and δ^{65}Cu data are for Pacific Deep Water samples between 1000 m and 3000 m at two stations (47° N, 152° W and 52° N, 152° W) in the North Pacific. Error bars are internal precision (2σ standard error), while grey bars depict the uncertainty of δ^{60}Ni and δ^{65}Cu analysis (2σ standard deviation).

4. Conclusions

In this study, we describe a new rapid procedure that utilizes automated chromatography for purifying Ni and Cu from seawater using a prepFAST-MC™ system for subsequent isotope analysis by Neptune MC-ICP-MS. This method effectively separates Ni and Cu from seawater matrix elements, thus avoiding spectral interferences and minimizing matrix effects during analysis. A nearly complete recovery of Ni and a quantitative recovery of Cu are achieved. The total procedural blanks were 0.33 ± 0.24 ng for Ni and 0.42 ± 0.18 ng for Cu, which are negligible for seawater Ni and Cu isotope analysis. The methods were further validated using seawater samples from the US GEOTRACES GP15 cruise. Purification of these samples by either the prepFAST or a manual column purification method, followed by MC-ICP-MS analysis generated equivalent δ^{60}Ni and δ^{65}Cu results. Repeated analysis of purified seawater samples indicates an overall uncertainty of 0.07 ‰ for δ^{60}Ni and 0.09 ‰ for δ^{65}Cu. Beyond this comparison, new data from the South Pacific show obvious Ni isotope fractionation in the upper ocean, whereas δ^{65}Cu remains similar throughout the water column. We anticipate that our method will encourage researchers to automate the chromatography of more isotope systems in the future. In particular, we note that Fe, Zn, and Cd are all eluted in a single fraction using the methods described here, and they can all be purified using the AG-MP1 resin employed here. This suggests that this method could possibly be expanded to purify those important elements from seawater for isotope analysis.

CRediT authorship contribution statement

Xiaopeng Bian: Writing – review & editing, Writing – original draft, Validation, Software, Methodology, Investigation, Conceptualization. **Shun-Chung Yang:** Writing – review & editing, Validation, Methodology, Investigation. **Robert J. Raad:** Writing – review & editing, Methodology, Investigation. **Nicholas J. Hawco:** Writing – review & editing, Resources, Investigation. **Jude Sakowski:** Writing – review & editing, Software, Methodology. **Kuo-Fang Huang:** Writing – review & editing, Resources. **Kyeong Pil Kong:** Writing – review & editing, Investigation. **Tim M. Conway:** Writing – review & editing, Resources. **Seth G. John:** Writing – review & editing, Supervision, Software, Funding acquisition, Conceptualization.

Declaration of competing interest

The authors declare the following financial interests/personal relationships which may be considered as potential competing interests. Jude Sakowski reports a relationship with Elemental Scientific, Inc. that includes: employment.

Data availability

Data will be made available on request.

Acknowledgments

We thank all the scientists, graduate students, and supertechs participating in the GEOTRACES GP15 cruise for sample collection, as

well as captain and crew of the R/V Roger Revelle RR 1814–1815 and R/V Falkor. We thank Dr. Simon V. Hohl for reviewing the draft of this manuscript and providing constructive comments. This manuscript greatly benefitted from the reviewing of the Editor and one anonymous reviewer. We thank Katherine Barbeau for use of GO-FLO bottles on SCOPE-Falkor. We thank Dave Wiederin and Paul Field from ESI for their help during the method development. We thank Ethan Goddard for technical assistance at USF. This study was supported by National Science Foundation award OCE1736896 to SGJ; OCE1737136 to TMC; and the Simons Foundation award 426570SP to SGJ.

Appendix A. Supplementary data

Supplementary data to this article can be found online at https://doi.org/10.1016/j.aca.2024.342753.

References

[1] F.M.M. Morel, A.J. Milligan, M.A. Saito, Marine bioinorganic chemistry: the role of trace metals in the oceanic cycles of major nutrients, Treatise Geochem. 6 (2003) 625.

[2] F.M.M. Morel, N.M. Price, The biogeochemical cycles of trace metals in the oceans, Science 300 (2003) 944–947.

[3] T.M. Conway, T.J. Horner, Y. Plancherel, A.G. González, A decade of progress in understanding cycles of trace elements and their isotopes in the oceans, Chem. Geol. 580 (2021) 120381, https://doi.org/10.1016/j.chemgeo.2021.120381.

[4] R. Schlitzer, R.F. Anderson, E.M. Dodas, M. Lohan, W. Geibert, A. Tagliabue, A. Bowie, C. Jeandel, M.T. Maldonado, W.M. Landing, D. Cockwell, C. Abadie, W. Abouchami, E.P. Achterberg, A. Agather, A. Aguliar-Islas, H.M. van Aken, M. Andersen, C. Archer, M. Auro, H.J. de Baar, O. Baars, A.R. Baker, K. Bakker, C. Basak, M. Baskaran, N.R. Bates, D. Bauch, P. van Beek, M.K. Behrens, E. Black, K. Bluhm, L. Bopp, H. Bouman, K. Bowman, J. Bown, P. Boyd, M. Boye, E.A. Boyle, P. Branellec, L. Bridgestock, G. Brissebrat, T. Browning, K.W. Bruland, H. J. Brumsack, M. Brzezinski, C.S. Buck, K.N. Buck, K. Buesseler, A. Bull, E. Butler, P. Cai, P.C. Mor, D. Cardinal, C. Carlson, G. Carrasco, N. Casacuberta, K. L. Casciotti, M. Castrillejo, E. Chamizo, R. Chance, M.A. Charette, J.E. Chaves, H. Cheng, F. Chever, M. Christl, T.M. Church, I. Closset, A. Colman, T.M. Conway, D. Cossa, P. Croot, J.T. Cullen, G.A. Cutter, C. Daniels, F. Dehairs, F. Deng, H. T. Dieu, B. Duggan, G. Dulaquais, C. Dumousseaud, Y. Echegoyen-Sanz, R. L. Edwards, M. Ellwood, E. Fahrbach, J.N. Fitzsimmons, A. Russell Flegal, M. Q. Fleisher, T. van de Flierdt, M. Frank, J. Friedrich, F. Fripiat, H. Fröllje, S.J. G. Galer, T. Gamo, R.S. Ganeshram, J. Garcia-Orellana, E. Garcia-Solsona, M. Gault-Ringold, E. George, L.J.A. Gerringa, M. Gilbert, J.M. Godoy, S. L. Goldstein, S.R. Gonzalez, K. Grissom, C. Hammerschmidt, A. Hartman, C. S. Hassler, E.C. Hathorne, M. Hatta, N. Hawco, C.T. Hayes, L.E. Heimbürger, J. Helgoe, M. Heller, G.M. Henderson, P.B. Henderson, S. van Heuven, P. Ho, T. J. Horner, Y.T. Hsieh, K.F. Huang, M.P. Humphreys, K. Isshiki, J.E. Jacquot, D. J. Janssen, W.J. Jenkins, S. John, E.M. Jones, J.L. Jones, D.C. Kadko, R. Kayser, T. C. Kenna, R. Khondoker, T. Kim, L. Kipp, J.K. Klar, M. Klunder, S. Kretschmer, Y. Kumamoto, P. Laan, M. Labatut, F. Lacan, P.J. Lam, M. Lambelet, C.H. Lamborg, F.A.C. Le Moigne, E. Le Roy, O.J. Lechtenfeld, J.M. Lee, P. Lherminier, S. Little, M. López-Lora, Y. Lu, P. Masque, E. Mawji, C.R. Mcclain, C. Measures, S. Mehic, J. L.M. Barraqueta, P. van der Merwe, R. Middag, S. Mieruch, A. Milne, T. Minami, J. W. Moffett, G. Moncoiffe, W.S. Moore, P.J. Morris, P.L. Morton, Y. Nakaguchi, N. Nakayama, J. Niedermiller, J. Nishioka, A. Nishiuchi, A. Noble, H. Obata, S. Ober, D.C. Ohnemus, J. van Ooijen, J. O'Sullivan, S. Owens, K. Pahnke, M. Paul, F. Pavia, L.D. Pena, B. Peters, F. Planchon, H. Planquette, C. Pradoux, V. Puigcorbé, P. Quay, F. Queroue, A. Radic, S. Rauschenberg, M. Rehkämper, R. Rember, T. Remenyi, J.A. Resing, J. Rickli, S. Rigaud, M.J.A. Rijkenberg, S. Rintoul, L. F. Robinson, M. Roca-Martí, V. Rodellas, T. Roeske, J.M. Rolison, M. Rosenberg, S. Roshan, M.M. Rutgers van der Loeff, E. Ryabenko, M.A. Saito, L.A. Salt, V. Sanial, G. Sarthou, C. Schallenberg, U. Schauer, H. Scher, C. Schlosser, B. Schnetger, P. Scott, P.N. Sedwick, I. Semiletov, R. Shelley, R.M. Sherrell, A. M. Shiller, D.M. Sigman, S.K. Singh, H.A. Slagter, E. Slater, W.M. Smethie, H. Snaith, Y. Sohrin, B. Sohst, J.E. Sonke, S. Speich, R. Steinfeldt, G. Stewart, T. Stichel, C.H. Stirling, J. Stutsman, G.J. Swarr, J.H. Swift, A. Thomas, K. Thorne, C.P. Till, R. Till, A.T. Townsend, E. Townsend, R. Tuerena, B.S. Twining, D. Vance, S. Velazquez, C. Venchiarutti, M. Villa-Alfageme, S.M. Vivancos, A.H.L. Voelker, B. Wake, M.J. Warner, R. Watson, E. van Weerlee, M. Alexandra Weigand, Y. Weinstein, D. Weiss, A. Wisotzki, E.M.S. Woodward, J. Wu, Y. Wu, K. Wuttig, N. Wyatt, Y. Xiang, R.C. Xie, Z. Xue, H. Yoshikawa, J. Zhang, P. Zhang, Y. Zhao, L. Zheng, X.Y. Zheng, M. Zieringer, L.A. Zimmer, P. Ziveri, P. Zunino, C. Zurbrick, The GEOTRACES intermediate data product 2017, Chem. Geol. 493 (2018) 210–223, https://doi.org/10.1016/j.chemgeo.2018.05.040.

[5] V. Cameron, D. Vance, Heavy nickel isotope compositions in rivers and the oceans, Geochem. Cosmochim. Acta 128 (2014) 195–211, https://doi.org/10.1016/j.gca.2013.12.007.

[6] T.M. Conway, S.G. John, The biogeochemical cycling of zinc and zinc isotopes in the North Atlantic Ocean, Global Biogeochem. Cycles 28 (2014) 1111–1128, https://doi.org/10.1002/2014GB004862.

[7] T.M. Conway, S.G. John, Biogeochemical cycling of cadmium isotopes along a high-resolution section through the North Atlantic Ocean, Geochem. Cosmochim. Acta 148 (2015) 269–283, https://doi.org/10.1016/j.gca.2014.09.032.

[8] S.G. John, J. Helgoe, E. Townsend, Biogeochemical cycling of Zn and Cd and their stable isotopes in the eastern tropical South Pacific, Mar. Chem. 201 (2018) 256–262, https://doi.org/10.1016/j.marchem.2017.06.001.

[9] S.H. Little, C. Archer, A. Milne, C. Schlosser, E.P. Achterberg, M.C. Lohan, D. Vance, Paired dissolved and particulate phase Cu isotope distributions in the South Atlantic, Chem. Geol. 502 (2018) 29–43, https://doi.org/10.1016/j.chemgeo.2018.07.022.

[10] S. Takano, M. Tanimizu, T. Hirata, Y. Sohrin, Isotopic constraints on biogeochemical cycling of copper in the ocean, Nat. Commun. 5 (2014) 1–7, https://doi.org/10.1038/ncomms6663.

[11] S.-C. Yang, R.L. Kelly, X. Bian, T.M. Conway, K.F. Huang, T.Y. Ho, J.A. Neibauer, R. G. Keil, J.W. Moffett, S.G. John, Lack of redox cycling for nickel in the water column of the Eastern tropical north pacific oxygen deficient zone: insight from dissolved and particulate nickel isotopes, Geochem. Cosmochim. Acta 309 (2021) 235–250, https://doi.org/10.1016/j.gca.2021.07.004.

[12] C. Archer, D. Vance, A. Milne, M.C. Lohan, The oceanic biogeochemistry of nickel and its isotopes: new data from the South Atlantic and the Southern Ocean biogeochemical divide, Earth Planet Sci. Lett. 535 (2020) 116118, https://doi.org/10.1016/j.epsl.2020.116118.

[13] S.H. Little, D. Vance, C. Walker-Brown, W.M. Landing, The oceanic mass balance of copper and zinc isotopes, investigated by analysis of their inputs, and outputs to ferromanganese oxide sediments, Geochem. Cosmochim. Acta 125 (2014) 673–693, https://doi.org/10.1016/j.gca.2013.07.046.

[14] S. Takano, M. Tanimizu, T. Hirata, K.C. Shin, Y. Fukami, K. Suzuki, Y. Sohrin, A simple and rapid method for isotopic analysis of nickel, copper, and zinc in seawater using chelating extraction and anion exchange, Anal. Chim. Acta 967 (2017) 1–11, https://doi.org/10.1016/j.aca.2017.03.010.

[15] D. Vance, S.H. Little, C. Archer, V. Cameron, M.B. Andersen, M.J.A. Rijkenberg, T. W. Lyons, The oceanic budgets of nickel and zinc isotopes: the importance of sulfdic environments as illustrated by the Black Sea, Phil. Trans. Math. Phys. Eng. Sci. 374 (2016), https://doi.org/10.1098/rsta.2015.0294.

[16] S.-C. Yang, N.J. Hawco, P. Pinedo-González, X. Bian, K.F. Huang, R. Zhang, S. G. John, A new purification method for Ni and Cu stable isotopes in seawater provides evidence for widespread Ni isotope fractionation by phytoplankton in the North Pacific, Chem. Geol. 547 (2020) 119662, https://doi.org/10.1016/j.chemgeo.2020.119662.

[17] T.M. Conway, A.D. Rosenberg, J.F. Adkins, S.G. John, A new method for precise determination of iron, zinc and cadmium stable isotope ratios in seawater by double-spike mass spectrometry, Anal. Chim. Acta 793 (2013) 44–52, https://doi.org/10.1016/j.aca.2013.07.025.

[18] E.R. Ciscato, T.R.R. Bontognali, D. Vance, Nickel and its isotopes in organic-rich sediments: implications for oceanic budgets and a potential record of ancient seawater, Earth Planet Sci. Lett. 494 (2018) 239–250, https://doi.org/10.1016/j.epsl.2018.04.061.

[19] Z. He, C. Archer, S. Yang, D. Vance, Sedimentary cycling of zinc and nickel and their isotopes on an upwelling margin: implications for oceanic budgets and paleoenvironment proxies, Geochem. Cosmochim. Acta 343 (2023) 84–97, https://doi.org/10.1016/j.gca.2022.12.026.

[20] S.H. Little, C. Archer, J. McManus, J. Najorka, A.V. Wegorzewski, D. Vance, Towards balancing the oceanic Ni budget, Earth Planet Sci. Lett. 547 (2020) 116461, https://doi.org/10.1016/j.epsl.2020.116461.

[21] S. Fleischmann, J. Du, A. Chatterjee, J. McManus, S.D. Iyer, A. Amonkar, D. Vance, The nickel output to abyssal pelagic manganese oxides: a balanced elemental and isotope budget for the oceans, Earth Planet Sci. Lett. 619 (2023) 118301, https://doi.org/10.1016/j.epsl.2023.118301.

[22] N. Lemaitre, J. Du, G.F. de Souza, C. Archer, D. Vance, The essential bioactive role of nickel in the oceans: evidence from nickel isotopes, Earth Planet Sci. Lett. 584 (2022) 117513, https://doi.org/10.1016/j.epsl.2022.117513.

[23] I. Baconnais, O. Rouxel, G. Dulaquais, M. Boye, Determination of the copper isotope composition of seawater revisited: a case study from the Mediterranean Sea, Chem. Geol. 511 (2019) 465–480, https://doi.org/10.1016/j.chemgeo.2018.09.009.

[24] C.M. Thompson, M.J. Ellwood, Dissolved copper isotope biogeochemistry in the tasman Sea, SW pacific ocean, Mar. Chem. 165 (2014) 1–9, https://doi.org/10.1016/j.marchem.2014.06.009.

[25] D. Vance, C. Archer, J. Bermin, J. Perkins, P.J. Statham, M.C. Lohan, M.J. Ellwood, R.A. Mills, The copper isotope geochemistry of rivers and the oceans, Earth Planet Sci. Lett. 274 (2008) 204–213, https://doi.org/10.1016/j.epsl.2008.07.026.

[26] X.K. Zhu, Y. Guo, R.J.P. Williams, R.K. O'Nions, A. Matthews, N.S. Belshaw, G. W. Canters, E.C. de Waal, U. Weser, B.K. Burgess, B. Salvato, Mass fractionation processes of transition metal isotopes, Earth Planet Sci. Lett. 200 (2002) 47–62, https://doi.org/10.1016/S0012-821X(02)00615-5.

[27] T.J. Horner, S.H. Little, T.M. Conway, J.R. Farmer, J.E. Hertzberg, D.J. Janssen, A. J.M. Lough, J.L. McKay, A. Tessin, S.J.G. Galer, S.L. Jaccard, F. Lacan, A. Paytan, K. Wuttig, GEOTRACES–PAGES biological productivity working group members, bioactive trace metals and their isotopes as paleoproductivity proxies: an assessment using GEOTRACES-Era data, Global Biogeochem. Cycles 35 (2021), https://doi.org/10.1029/2020GB006814.

[28] J. Irrgeher, T. Prohaska, Application of non-traditional stable isotopes in analytical ecogeochemistry assessed by MC ICP-MS - a critical review, Anal. Bioanal. Chem. 408 (2016) 369–385, https://doi.org/10.1007/s00216-015-9025-3.

[29] L. Yang, Accurate and precise determination of isotopic ratios by MC-ICP-MS: a review, Mass Spectrom. Rev. 28 (2009) 990–1011, https://doi.org/10.1002/mas.20251.
[30] R.M. Wang, C. Archer, A.R. Bowie, D. Vance, Zinc and nickel isotopes in seawater from the Indian Sector of the Southern Ocean: the impact of natural iron fertilization versus Southern Ocean hydrography and biogeochemistry, Chem. Geol. 511 (2019) 452–464, https://doi.org/10.1016/j.chemgeo.2018.09.010.
[31] S.J. Romaniello, M.P. Field, H.B. Smith, G.W. Gordon, M.H. Kim, A.D. Anbar, Fully automated chromatographic purification of Sr and Ca for isotopic analysis, J. Anal. Atomic Spectrom. 30 (2015) 1906–1912.
[32] T.G. Enge, M.P. Field, D.F. Jolley, H. Ecroyd, M.H. Kim, A. Dosseto, An automated chromatography procedure optimized for analysis of stable Cu isotopes from biological materials, J. Anal. Atomic Spectrom. 31 (2016) 2023–2030, https://doi.org/10.1039/c6ja00120c.
[33] A.M. Wefing, J. Arps, P. Blaser, C. Wienberg, D. Hebbeln, N. Frank, High precision U-series dating of scleractinian cold-water corals using an automated chromatographic U and Th extraction, Chem. Geol. 475 (2017) 140–148, https://doi.org/10.1016/j.chemgeo.2017.10.036.
[34] A. Retzmann, T. Zimmermann, D. Pröfrock, T. Prohaska, J. Irrgeher, A fully automated simultaneous single-stage separation of Sr, Pb, and Nd using DGA Resin for the isotopic analysis of marine sediments, Anal. Bioanal. Chem. 409 (2017) 5463–5480, https://doi.org/10.1007/s00216-017-0468-6.
[35] S.C. Metzger, B.W. Ticknor, K.T. Rogers, D. Bostick, E.H. Mcbay, C.R. Hexel, Automated separation of Uranium and Plutonium from Environmental Swipe samples for multiple collector inductively coupled plasma mass spectrometry, Anal. Chem. (2018), https://doi.org/10.1021/acs.analchem.8b02095.
[36] E. de la Vega, G.L. Foster, M.A. Martínez-Botí, E. Anagnostou, M.P. Field, M. H. Kim, P. Watson, P.A. Wilson, Automation of boron chromatographic purification for δ11B analysis of coral aragonite, Rapid Commun. Mass Spectrom. 34 (2020) 1–11, https://doi.org/10.1002/rcm.8762.
[37] M.P. Field, T.M. Conway, B.A. Summers, N. Saetveit, J.C. Sakowski, Automated processing of seawater samples for iron isotope ratio determination, in: GOLDSCHMIDT, 2019. https://goldschmidtabstracts.info/2019/990.pdf.
[38] B. Mahan, R.S. Chung, D.L. Pountney, F. Moynier, S. Turner, Isotope metallomics approaches for medical research, Cell. Mol. Life Sci. 77 (2020) 3293–3309, https://doi.org/10.1007/s00018-020-03484-0.
[39] F. Albarède, Metal stable isotopes in the human Body: a tribute of geochemistry to medicine, Elements 11 (2015) 265–269, https://doi.org/10.2113/gselements.11.4.265.
[40] Y.K. Tanaka, T. Hirata, Stable isotope composition of metal elements in biological samples as tracers for element metabolism, Anal. Sci. 34 (2018) 645–655, https://doi.org/10.2116/analsci.18SBR02.
[41] S.G. John, R.L. Kelly, X. Bian, F. Fu, M.I. Smith, N.T. Lanning, H. Liang, B. Pasquier, E.A. Seelen, M. Holzer, The biogeochemical balance of oceanic nickel cycling, Nat. Geosci. 15 (2022) 906–912.
[42] G.A. Cutter, K. Casciotti, P. Croot, W. Geibert, L.-E. Heimbürger, M.C. Lohan, H. Planquette, T. van de Flierdt, Sampling and Sample-Handling Protocols for GEOTRACES Cruises, 2017, Version 3.0.
[43] P. Pinedo-González, N.J. Hawco, R.M. Bundy, E.V. Armbrust, M.J. Follows, B. B. Cael, A.E. White, S. Ferrón, D.M. Karl, S.G. John, Anthropogenic Asian aerosols provide Fe to the North Pacific ocean, Proc. Natl. Acad. Sci. U.S.A. 117 (2020) 27862–27868, https://doi.org/10.1073/pnas.2010315117.
[44] N.J. Hawco, S.C. Yang, R.K. Foreman, C.P. Funkey, M. Dugenne, A.E. White, S. T. Wilson, R.L. Kelly, X. Bian, K.F. Huang, D.M. Karl, S.G. John, Metal isotope signatures from lava-seawater interaction during the 2018 eruption of Kīlauea, Geochem. Cosmochim. Acta 282 (2020) 340–356, https://doi.org/10.1016/j.gca.2020.05.005.
[45] S.-C. Yang, L. Welter, A. Kolatkar, J. Nieva, K.R. Waitman, K.-F. Huang, W.-H. Liao, S. Takano, W.M. Berelson, A.J. West, P. Kuhn, S.G. John, A new anion exchange purification method for Cu stable isotopes in blood samples, Anal. Bioanal. Chem. (2018), https://doi.org/10.1007/s00216-018-1498-4.
[46] C. Siebert, T.F. Nägler, J.D. Kramers, Determination of molybdenum isotope fractionation by double-spike multicollector inductively coupled plasma mass spectrometry, G-cubed 2 (2001), https://doi.org/10.1029/2000GC000124.
[47] J. Bermin, D. Vance, C. Archer, P.J. Statham, The determination of the isotopic composition of Cu and Zn in seawater, Chem. Geol. 226 (2006) 280–297, https://doi.org/10.1016/j.chemgeo.2005.09.025.
[48] L. Gall, H. Williams, C. Siebert, A. Halliday, Determination of mass-dependent variations in nickel isotope compositions using double spiking and MC-ICPMS, J. Anal. Atomic Spectrom. 27 (2012) 137–145, https://doi.org/10.1039/c1ja10209e.
[49] F.J. Flanagan, US Geological Survey standards—II. First compilation of data for the new USGS rocks, Geochem. Cosmochim. Acta 33 (1969) 81–120.
[50] D. Hare, C. Austin, P. Doble, Quantification strategies for elemental imaging of biological samples using laser ablation-inductively coupled plasma-mass spectrometry, Analyst 137 (2012) 1527–1537.
[51] N. Dauphas, S.G. John, O. Rouxel, Iron isotope systematics, Rev. Mineral. Geochem. 82 (2017) 415–510, https://doi.org/10.2138/rmg.2017.82.11.
[52] S. Weyer, J.B. Schwieters, High precision Fe isotope measurements with high mass resolution MC-ICPMS, Int. J. Mass Spectrom. 226 (2003) 355–368, https://doi.org/10.1016/S1387-3806(03)00078-2.
[53] K.J. Orians, E.A. Boyle, K.W. Bruland, Dissolved titanium in the open ocean, Nature 348 (1990) 322–325.
[54] V.L. Dressler, D. Pozebon, A. Matusch, J.S. Becker, Micronebulization for trace analysis of lanthanides in small biological specimens by ICP-MS, Int. J. Mass Spectrom. 266 (2007) 25–33, https://doi.org/10.1016/j.ijms.2007.06.018.
[55] E. Frères, D. Weis, K. Newman, M. Amini, K. Gordon, Oxide Formation and instrumental mass bias in MC-ICP-MS: an isotopic case study of Neodymium, Geostand. Geoanal. Res. 45 (2021) 501–523, https://doi.org/10.1111/ggr.12381.
[56] J.B. Chapman, T.F.D. Mason, D.J. Weiss, B.J. Coles, J.J. Wilkinson, Chemical separation and isotopic variations of Cu and Zn from five geological reference materials, Geostand. Geoanal. Res. 30 (2006) 5–16, https://doi.org/10.1111/j.1751-908x.2006.tb00907.x.
[57] M. Klaver, C.D. Coath, Obtaining accurate isotopic compositions with the double spike technique: practical considerations, Geostand. Geoanal. Res. 43 (2019) 5–22, https://doi.org/10.1111/ggr.12248.
[58] A.M. Posacka, D.M. Semeniuk, H. Whitby, C.M.G. Van Den Berg, J.T. Cullen, K. Orians, M.T. Maldonado, Dissolved copper (dCu) biogeochemical cycling in the subarctic Northeast Pacific and a call for improving methodologies, Mar. Chem. 196 (2017) 47–61, https://doi.org/10.1016/j.marchem.2017.05.007.
[59] M.E. Lagerström, M.P. Field, M. Séguret, L. Fischer, S. Hann, R.M. Sherrell, Automated on-line flow-injection ICP-MS determination of trace metals (Mn, Fe, Co, Ni, Cu and Zn) in open ocean seawater: application to the GEOTRACES program, Mar. Chem. 155 (2013) 71–80, https://doi.org/10.1016/j.marchem.2013.06.001.
[60] G. Wu, J.-M. Zhu, X. Wang, T.M. Johnson, Y. He, F. Huang, L.-X. Wang, S.-C. Lai, Nickel isotopic composition of the upper continental crust, Geochem. Cosmochim. Acta 332 (2022) 263–284, https://doi.org/10.1016/j.gca.2022.06.019.
[61] W. Li, S.E. Jackson, N.J. Pearson, O. Alard, B.W. Chappell, The Cu isotopic signature of granites from the Lachlan Fold Belt, SE Australia, Chem. Geol. 258 (2009) 38–49, https://doi.org/10.1016/j.chemgeo.2008.06.047.
[62] J.C.J. Petit, J. de Jong, L. Chou, N. Mattielli, Development of Cu and Zn isotope MC-ICP-MS measurements: application to suspended particulate matter and sediments from the scheldt estuary, Geostand. Geoanal. Res. 32 (2008) 149–166, https://doi.org/10.1111/j.1751-908X.2008.00867.x.
[63] T.W. May, R.H. Wiedmeyer, A table of polyatomic interferences in ICP-MS, ATOMIC SPECTROSCOPY-NORWALK CONNECTICUT- 19 (1998) 150–155.